

# Wear and Corrosion Resistance of Pure Titanium Subjected to Aluminization and Coated with a Microarc Oxidation Ceramic Coating

Chia-Jung Hu\*, Po-Han Chiu

Dept. of Materials Engineering, Tatung University, 40 Chungshan N. Road, 3rd Sec., Taipei 104, Taiwan

\*E-mail: [cjhu@ttu.edu.tw](mailto:cjhu@ttu.edu.tw)

Received: 16 February 2015 / Accepted: 3 March 2015 / Published: 23 March 2015

---

An Al<sub>2</sub>O<sub>3</sub> layer on hot-dip aluminized chemically pure titanium was successfully produced using microarc oxidation (MAO). The thickness of the Al<sub>2</sub>O<sub>3</sub> layer increased with the MAO duration. However, the growth rate of the Al<sub>2</sub>O<sub>3</sub> layer reached the maximum value after approximately 20 min of MAO. Samples undergoing MAO for 20 min exhibited the highest corrosion resistance in a 3.5 wt.% NaCl solution. The larger pore size on the surface of samples undergoing MAO for over 20 min accounted for the relatively poorer corrosion resistance. The thickness and hardness of the Al<sub>2</sub>O<sub>3</sub> layer are critical for its abrasion resistance. The wear resistance of the duplex coatings can be considerably improved by increasing the MAO duration, and this improvement is attributable to the increased MAO coating thickness. In this study, the samples undergoing MAO for 40 min yielded the highest wear resistance. After subsequent diffusion annealing, cracks in the Al<sub>3</sub>Ti layer, arising from the volume shrinkage caused by the Al<sub>3</sub>Ti formation, caused the corrosion resistance to be poor.

---

**Keywords:** Pure titanium; Hot-dip aluminum; Microarc oxidation; Al<sub>3</sub>Ti; Corrosion resistance; Wear resistance

## 1. INTRODUCTION

Improving car engine efficiency is vital for performance-related and ecological reasons, that is, for reducing fuel consumption and vehicular emissions. Reducing the mass of auxiliary units of the engine reduces the energy necessary to transmit the generated power. Therefore, titanium alloys with a high strength-to-weight ratio have been used in the valves of professional racing car engines. However, the poor tribological properties of titanium, arising from the hardness of titania coatings (550–1050 HV) [1, 2], affect the service life, even for titanium valves with abrasive ceramic overlay coatings, such as diamond-like carbon [3] and physical vapor deposition [4] coatings. Microarc oxidation

(MAO) is an electrochemical surface treatment that forms an extremely adhesive coating, which metallurgically bonds to the substrate [5-7]. MAO on aluminized titanium generates a thick alumina coating; the high hardness of this coating (1200–1800 HV) overcomes the low wear resistance of titanium alloys [8-10]. Hot-dip aluminizing involves pretreating the surfaces of samples and immersing them in molten aluminum or aluminum alloy baths for a specific duration, during which the liquid aluminum and the matrix metal interdiffuse. This method, frequently applied to stainless steels [11], carbon steels, and alloy steels [12, 13], improves corrosion, wear, and oxidation resistance at high temperatures. Aluminized and annealed titanium, which consists of an intermetallic inner layer and an alumina outer layer on titanium or titanium alloys, exhibits improved oxidation and corrosion resistance [14-16]. However, few studies have focused on increasing the wear and corrosion resistance of aluminized titanium. In this study, pure titanium was subjected to aluminization and coated with a microarc oxidation ceramic coating, and followed by annealing to form the composite layer, which consisted of a thick alumina outer layer, an aluminum intermediate layer, and an intermetallic inner layer on titanium substrate. This study assessed whether the duplex process of aluminizing titanium and applying an MAO ceramic coating increases the wear and corrosion resistance of pure titanium.

## 2. EXPERIMENTAL PROCEDURE

Rectangular samples (50 mm × 30 mm × 2 mm) of chemically pure titanium were used as the working electrodes. The samples were mechanically polished using waterproof abrasive paper up to 800 grit and ultrasonically degreased in acetone and distilled water. Prior to MAO, the samples were hot-dipped in molten aluminum for 2 min at a constant temperature of 720 °C, followed by air cooling. The aqueous electrolyte used in MAO contained 10 g/L NaAlO<sub>2</sub>. During MAO, the electrolytic solution in the stainless steel container (counter electrode) was maintained below 40 °C by using a chiller. A pulsed bipolar electrical source with a power of 12 kW was used. The treatment was conducted at a constant current mode: a current density of 10 A/dm<sup>2</sup> for the anode and 5 A/dm<sup>2</sup> for the cathode. The other electrical parameters were bipolar rectangular pulses at a frequency of 1000 Hz, a duty ratio of 0.32, and treatment durations of 10, 20, 30, and 40 min.

The phase and microstructure of the coatings were evaluated through X-ray diffraction (MAV Science M21X) and scanning electron microscopy (FESEM, SU8000), respectively. The thickness and arithmetic mean surface roughness (Ra) of the coatings were measured using an eddy current coating measurement gauge (Fisher Isoscope MP10-E) and a surface profilometer (Mitutoyo SJ-201), respectively. The microhardness (HV) was measured using a microhardness tester (Fischerscope HM 2000S) with a maximum indentation depth of 1 μm; the average microhardness at 5 points on the coating surface was recorded. The corrosion resistance of the MAO coating was evaluated through potentiodynamic polarization (Solartron SI 1287 electrochemical interface) in a 3.5 wt.% NaCl solution, with a saturated calomel electrode (SCE) used as the reference electrode. The friction coefficients were measured using a computer-controlled oscillating ball-on-disk tribometer (CSM TRN 01-05600) equipped with a tungsten carbide ball 6 mm in diameter. The measurement was conducted at a linear speed of 5 cm/s, track radius of 5 mm, and load of 5 N. After the tribological tests, the wear

track images were analyzed through SEM, and the surface profiles were measured using a stylus profiler (Veeco Metrology, Dektak 150) at a load of 3 mg. The wear volume was determined using the profiles from the wear track cross-section, and the specific wear rate  $K_s$  was calculated as  $K_s = \Delta V/(P \cdot d)$ , where  $P$  is the normal load (5 N),  $d$  is the sliding distance (200 m), and  $\Delta V$  is the wear volume, which is obtained by multiplying the wear depth, wear width, and track radius (5 mm).

### 3. RESULTS AND DISCUSSION

#### 3.1. Phase formation of MAO coatings on aluminized titanium

Prior to MAO, the samples were hot-dipped in molten aluminum at 720 °C for 2 min. Energy dispersive spectrometry (EDS) indicated that an approximately 50–60- $\mu\text{m}$  thick aluminum layer on pure titanium and an approximately 2- $\mu\text{m}$  thick  $\text{Al}_3\text{Ti}$  layer were present between the aluminum coating and the pure titanium substrate. After MAO of the aluminized titanium, XRD of the coating formed in the sodium aluminate electrolyte for 10, 20, 30, and 40 min showed  $\gamma\text{-Al}_2\text{O}_3$  and  $\alpha\text{-Al}_2\text{O}_3$  peaks (Fig. 1). A few peaks of  $\text{Al}_3\text{Ti}$  intermetallic compounds were found in the XRD of the coating formed using MAO for 10 min (Fig. 1b). Although the formation energy of  $\text{Al}_2\text{Ti}$  is lower than that of  $\text{Al}_3\text{Ti}$  [14, 15], only the  $\text{Al}_3\text{Ti}$  phase was observed during the interaction of the solid titanium and liquid aluminum. As indicated in Wang's report [16], the difference in formation energies between the product ( $\text{TiAl}_2$ ) and the reactant ( $\text{TiAl}_3$ ) drives  $\text{TiAl}_2$  formation. However, a  $\text{TiAl}_2$  layer cannot be formed because of the insufficiency of the driving force required to overcome the interfacial energy barriers in  $\text{TiAl}_2$  formation. A stable phase is absent in the diffusion zone when the driving force is insufficient to overcome the interfacial energy increase. Therefore, in this study,  $\text{TiAl}_2$  could not form a distinct layer because the temperature was not sufficiently high.

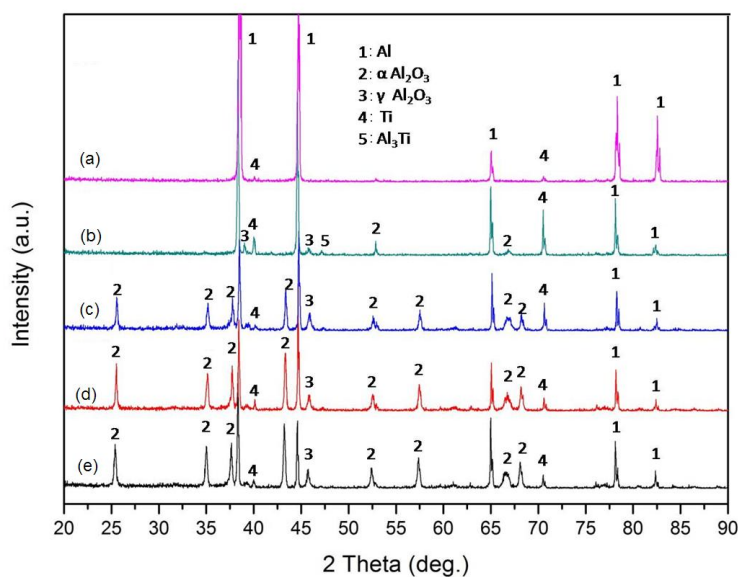


**Figure 1.** XRD patterns of (a) as-aluminized titanium and formed through subsequent MAO for (b) 10 min, (c) 20 min, (d) 30 min, and (e) 40 min.

In samples that underwent MAO for over 20 min, no other intermetallic phase except that of  $\text{Al}_3\text{Ti}$  was found in the surface of the coating, whereas more peaks of  $\alpha\text{-Al}_2\text{O}_3$  were found in the XRD of coatings oxidized for prolonged durations. The amount of  $\alpha\text{-Al}_2\text{O}_3$  in the MAO coatings increased with the MAO duration because of the stable structure of  $\alpha\text{-Al}_2\text{O}_3$ ; this observation is similar to previously reported results [17, 18]. However, metastable  $\gamma\text{-Al}_2\text{O}_3$  was still found in the coatings after prolonged MAO durations. Although the coating thickness increased with the MAO duration, the phase constituent of the coating appeared to be independent of the MAO duration when the oxidization duration was over 20 min (Fig. 1 and 2).

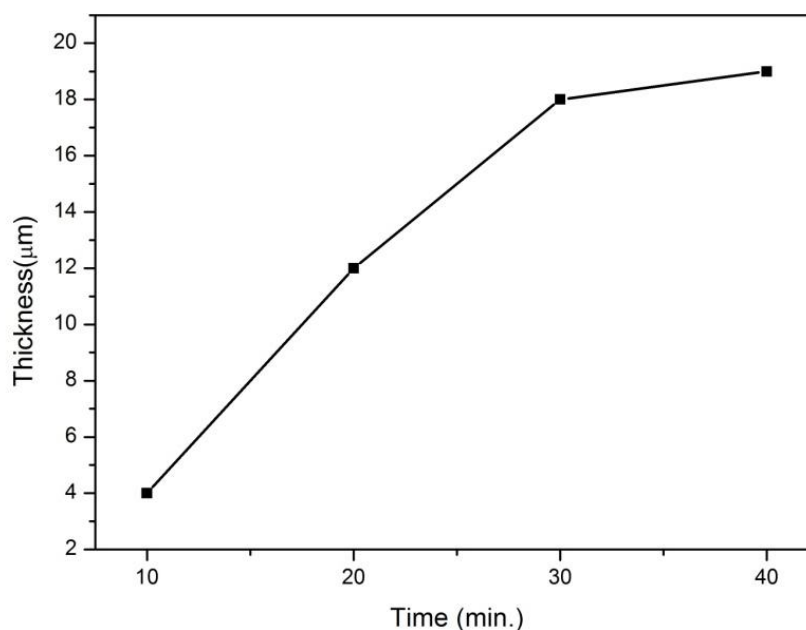


**Figure 2.** Thickness variation of the MAO coatings with MAO duration.

### 3.2. Properties of MAO coatings

As shown in Fig. 2, the MAO coating initially grew linearly for up to 20 min. After MAO for 20 min, the deposition rate monotonically decreased with the MAO duration; this observation is similar to previously reported results [19]. These results imply that beyond a certain oxidation duration, the coating thickness grows slowly. The same variation in the thickness of alumina coatings was observed in cross-sections of the coatings (Fig. 3). Prior to MAO, an approximately 2- $\mu\text{m}$ -thick  $\text{Al}_3\text{Ti}$  layer had formed between the aluminum coating and the pure titanium substrate during hot-dip aluminizing. After MAO for 10, 20, 30, and 40 min, the thickness of the  $\text{Al}_3\text{Ti}$  layer was nearly independent of the MAO duration, as illustrated in Fig. 3, and a typical porous inner layer was observed in the alumina coatings. As described by Xue [20], the lifetime of each spark (microarc) is  $<1$  ms, and the melt–solidification process in the microarc discharge zone is short. Therefore, the plasma discharge process hardly influenced the titanium alloy substrate, and the thickness of the intermetallic layer between the aluminum coating and the titanium substrate did not change after MAO.

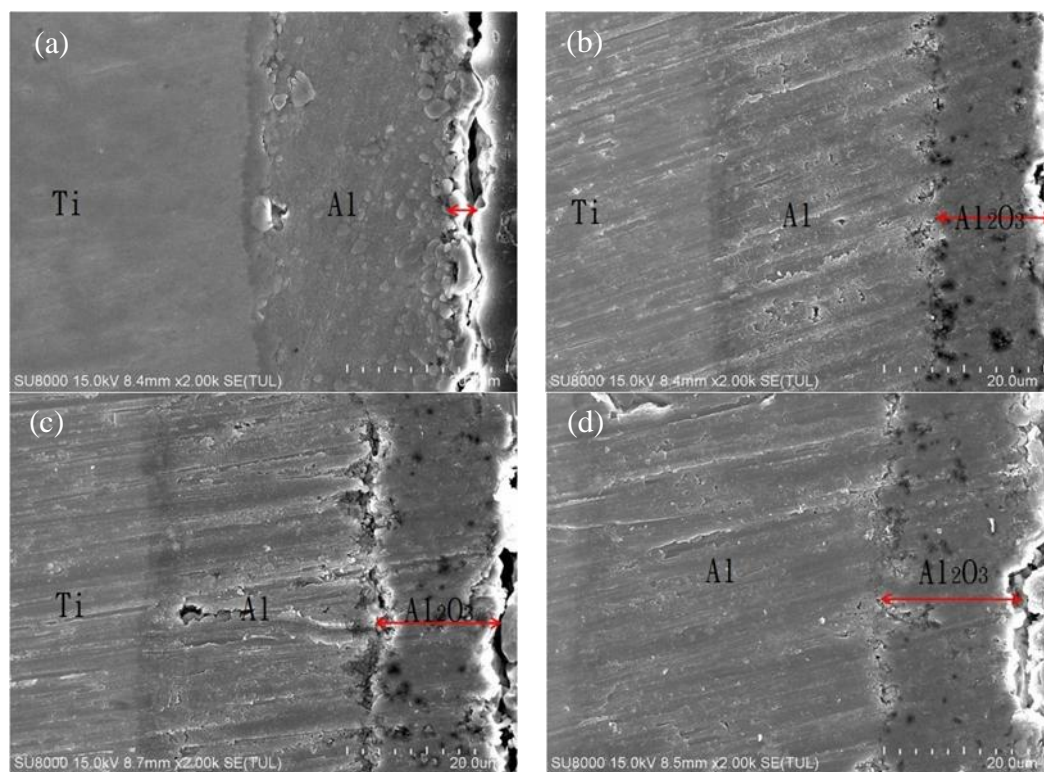


**Figure 3.** Cross-sectional SEM morphologies of the MAO coatings formed for (a) 10 min, (b) 20 min, (c) 30 min, and (d) 40 min.

A typical surface roughness variation of the MAO coating is shown in Fig. 4, which indicates that the roughness increased with the MAO duration. In particular, the roughness of the coating formed through 40 min of MAO was high because of the larger pores in its surface. This microstructure resulted in a slow increase in coating hardness after the MAO duration exceeded 30 min, as shown in Fig. 5. The hardness of the  $\text{Al}_2\text{O}_3$  layer increased with the MAO duration after the formation of the  $\alpha\text{-Al}_2\text{O}_3$  phase. The soft titanium substrate contributed to the low hardness in samples with thin MAO coatings, such as those formed for 10 min. The polarization curves measured in a 3.5 wt.% NaCl solution for the coated samples formed at different durations are shown in Fig. 6. The corrosion potential and current density, derived directly from the polarization curves through Tafel region extrapolation, are summarized in Table 1. The corrosion potential ( $E_{\text{corr}}$  versus SCE) of the MAO coating formed for 20 min was  $-0.468$  V, whereas the coatings formed for 10, 30, and 40 min exhibited a more negative corrosion potential ( $-0.58$ ,  $-0.579$ , and  $-0.648$  V, respectively). The corrosion rate of the coated samples is generally determined using the corrosion current density, which is mainly associated with the coating microstructure [21]. Table 1 clearly shows that the MAO coating formed for 20 min exhibited a much lower corrosion current density and a higher corrosion resistance than did those formed for 10, 30, and 40 min. The larger pore sizes on the surface of the coatings formed for over 20 min accounts for their poorer corrosion resistance. However, the MAO sample formed for over 20 min exhibited a lower corrosion current density than did the coating formed for 10 min and the as-aluminized sample.

**Table 1.** Corrosion properties of MAO coatings.

MAO time (min.)	Corrosion potential (V vs. SCE) (V)	Corrosion current density (A/cm <sup>2</sup> )
Substrate-Ti	-0.255	$1.16 \times 10^{-8}$
As-dipped HAD	-0.741	$3.55 \times 10^{-5}$
10	-0.580	$5.69 \times 10^{-8}$
20	-0.468	$2.39 \times 10^{-9}$
30	-0.579	$7.77 \times 10^{-9}$
40	-0.648	$1.70 \times 10^{-8}$

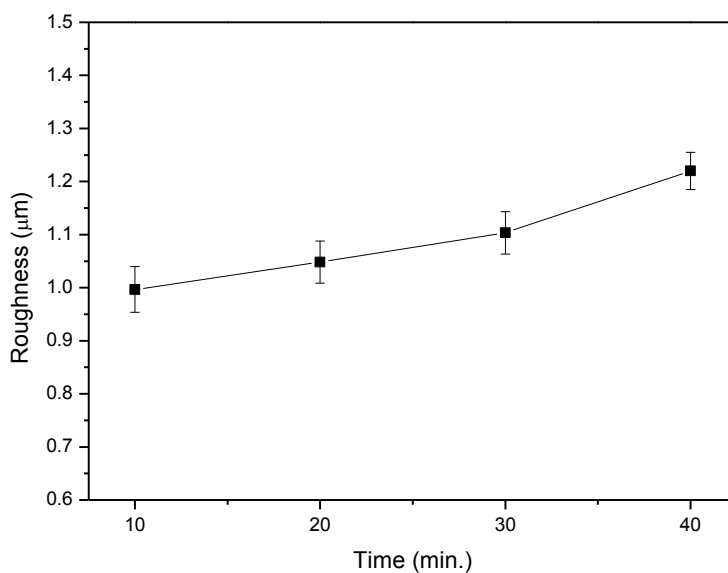


**Figure 4.** Roughness variation of the MAO coatings with MAO duration.

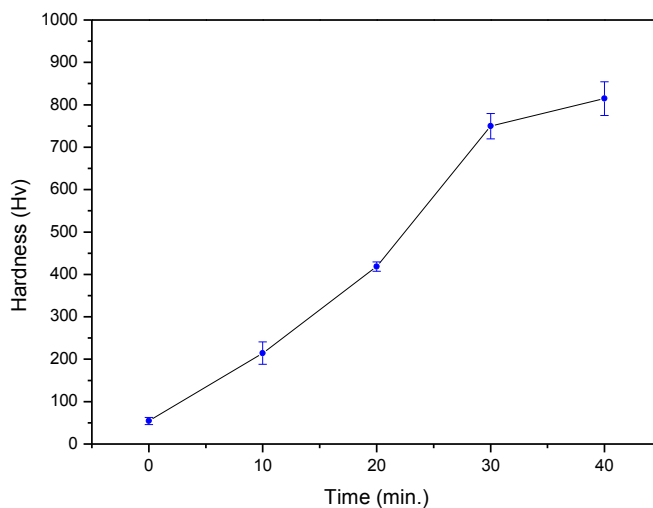


**Figure 5.** Hardness variation of the MAO coatings with MAO duration.

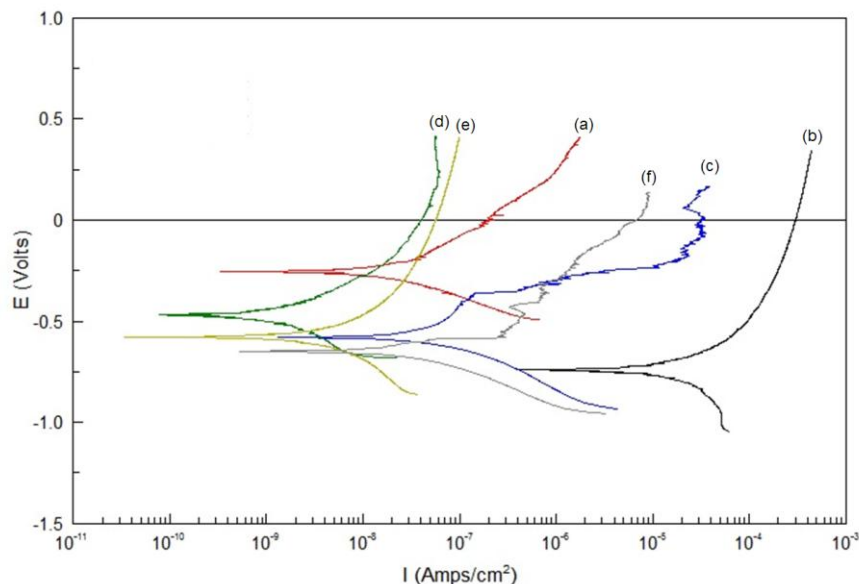


**Figure 6.** Polarization curves in 3.5 wt.% NaCl solution for (a) titanium substrate, (b) as-aluminized titanium, and titanium subjected to subsequent MAO for (c) 10 min, (d) 20 min, (e) 30 min, and (f) 40 min.

Fig. 7 depicts the friction coefficients of the pure titanium substrate and the MAO coatings formed for different durations. The friction coefficients of the MAO samples formed for over 20 min exhibited a lower and more stable variation than did those of the MAO sample formed for 10 min and the pure titanium substrate. The friction coefficient of the MAO coating formed for 10 min rapidly increased to approximately 0.6 over the initial sliding distance and steeply increased to approximately 0.85 after sliding 30 m. This unstable variation in the friction coefficient was caused by the detachment of the thin alumina layer, approximately 4  $\mu\text{m}$  thick, on the sample surface. However, after sliding 50 m, the MAO coating formed for 10 min exhibited a lower and more stable friction coefficient than that of the pure titanium substrate. In general, MAO coatings provided superior wear protection. SEM images of the wear track revealed that wear widths decreased with the MAO duration, because the MAO coating thickness increased (Fig. 8). Using the measured wear widths and depths (Fig. 9), specific wear rates were calculated for the pure titanium substrate and MAO coatings (Table 2). The calculated results yielded specific wear rates of approximately  $7.7 \times 10^{-4}$ ,  $3.4 \times 10^{-4}$ ,  $0.47 \times 10^{-4}$ ,  $0.39 \times 10^{-4}$ , and  $0.29 \times 10^{-4} \text{ mm}^3/\text{N}\cdot\text{m}$  for the substrate and MAO coatings formed for 10, 20, 30, and 40 min, respectively. The thickness and hardness of the  $\text{Al}_2\text{O}_3$  layer is critical in abrasion resistance. The wear resistance of the coatings can be considerably improved by increasing the MAO duration because of the consequent increase in the MAO coating thickness. The MAO coatings formed for 40 min yielded the highest wear resistance.

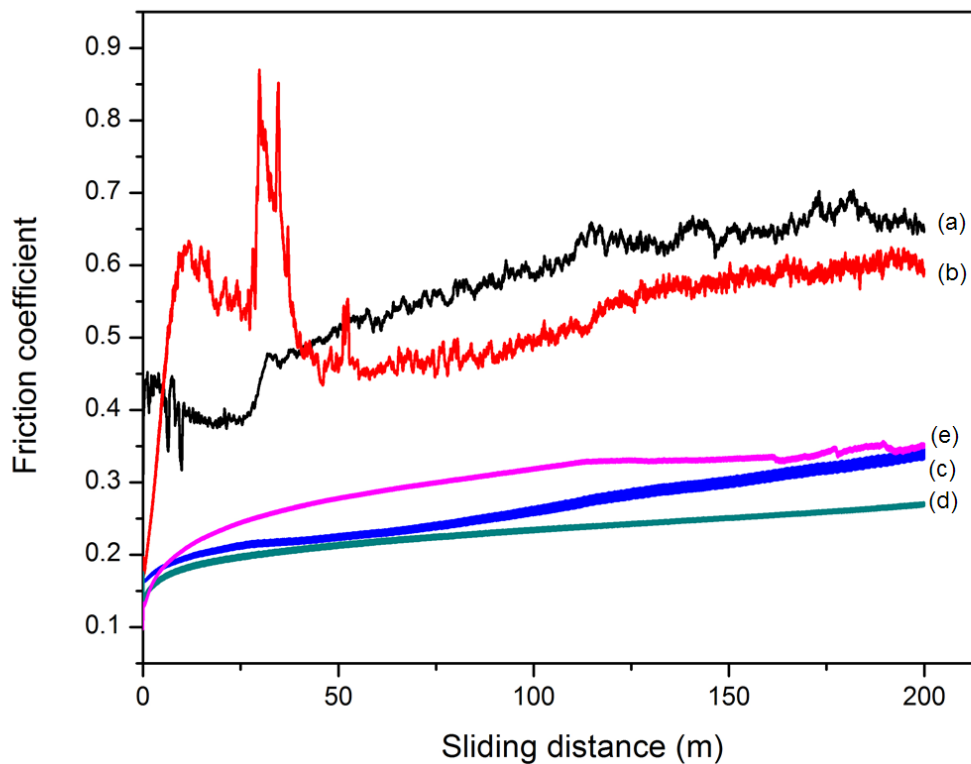


**Figure 7.** Friction coefficient of (a) titanium substrate and MAO coatings formed for (b) 10 min, (c) 20 min, (d) 30 min, and (e) 40 min.

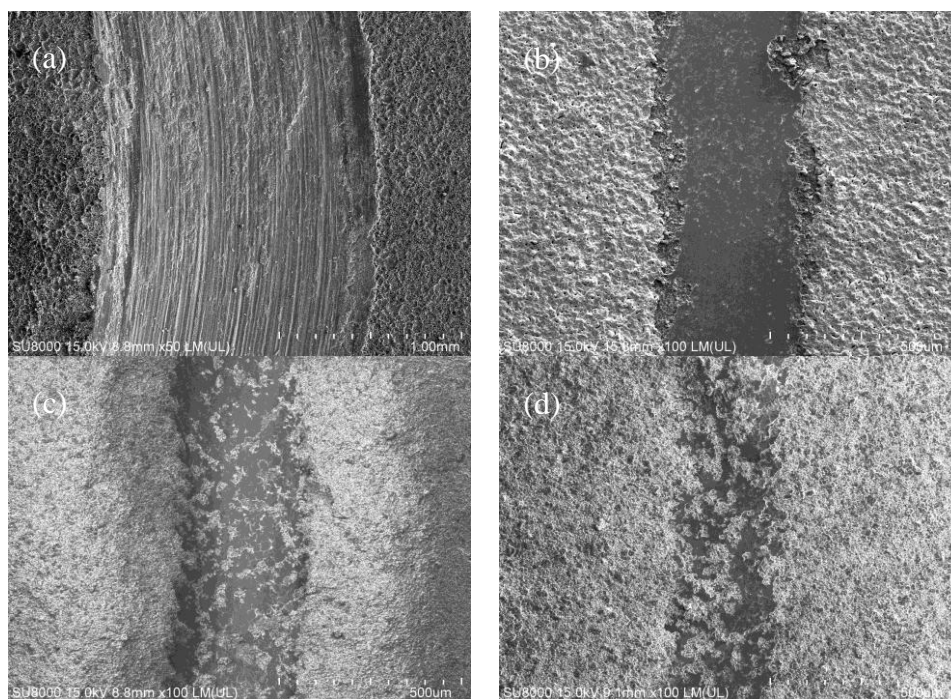


**Figure 8.** Wear tracks of MAO coatings formed on hot-dip aluminized titanium for MAO durations of (a) 10 min, (b) 20 min, (c) 30 min, and (d) 40 min.

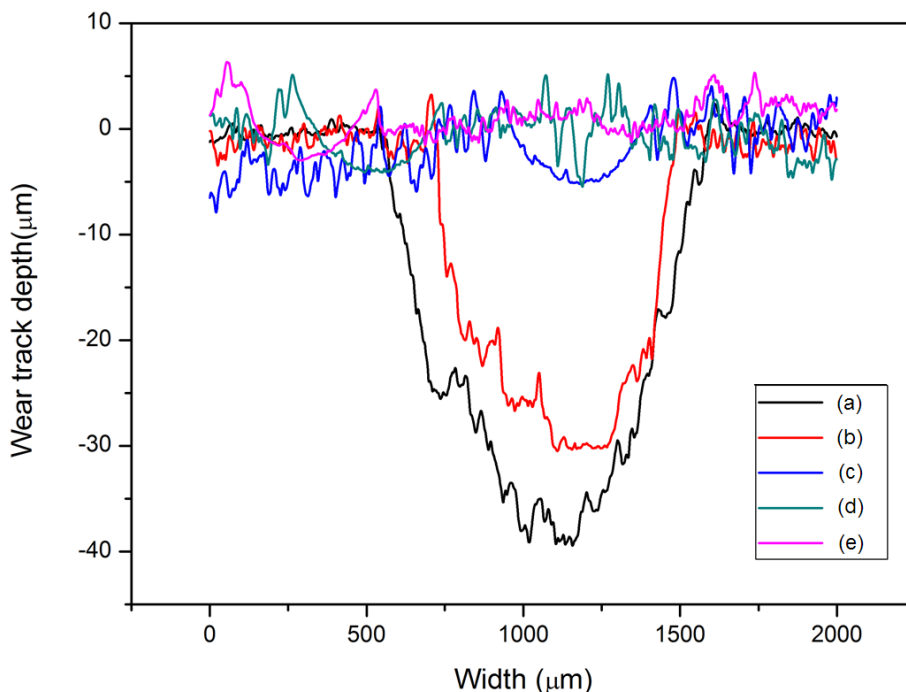


**Figure 9.** Surface profiles of the samples after tribological tests for (a) titanium substrate and hot-dip aluminized titanium formed through MAO for (b) 10 min, (c) 20 min, (d) 30 min, and (e) 40 min.

**Table 2.** Specific wear rate for pure titanium substrate and MAO coatings.

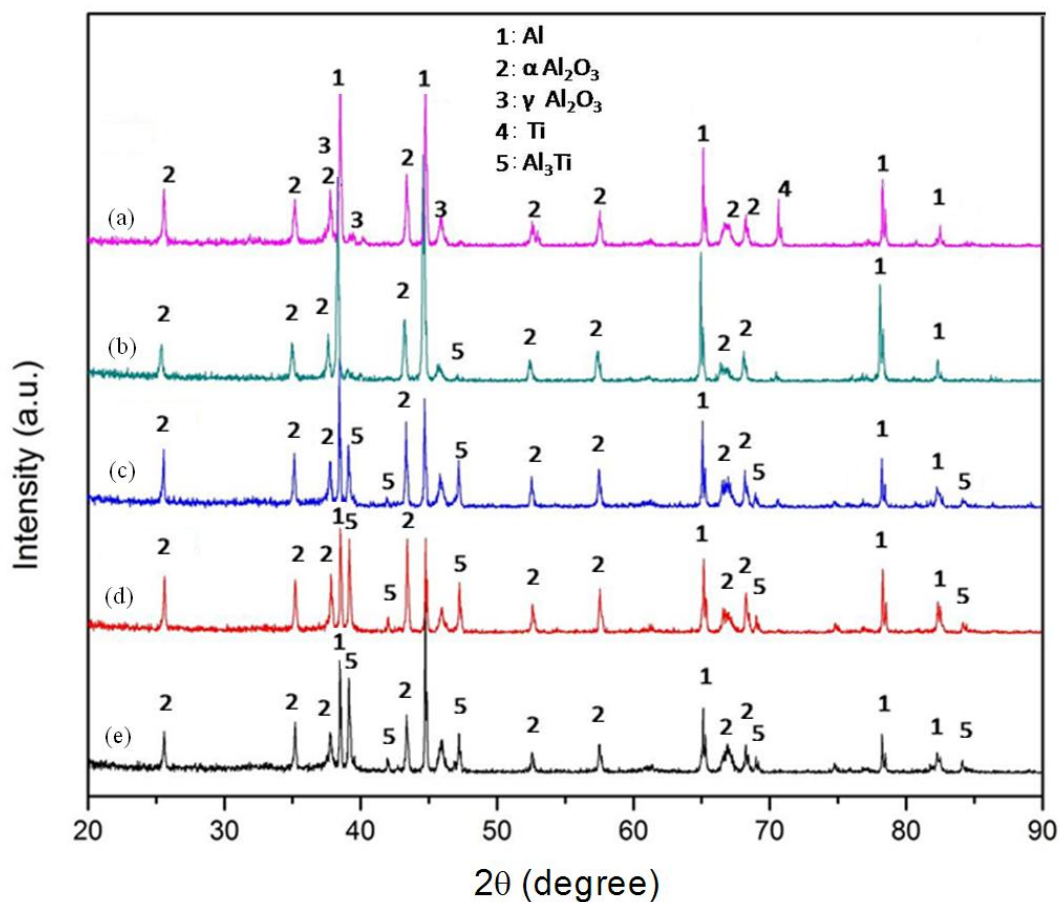
MAO time (min.)	Wear width (μm)	Sample wear rate, $K_s$ ( $\text{mm}^3/\text{N m}$ )
Substrate	1076.5	$7.75 \times 10^{-4}$
10	792	$3.41 \times 10^{-4}$
20	549.4	$0.47 \times 10^{-4}$
30	479.8	$0.39 \times 10^{-4}$
40	433.2	$0.29 \times 10^{-4}$

Note:  $K_s = \Delta V / (P \cdot d)$ , where P is the normal load of 5N, d is the sliding distance of 200 m, and  $\Delta V$  (wear volume) was calculated by wear depth, wear width, and the track radius of 5 mm.

### 3.3. Effect of diffusion annealing on MAO coatings

Subsequent to MAO coating, diffusion annealing was performed to facilitate the formation of the intermetallic layer. Fig. 10 shows XRD patterns of the coatings when diffusion-treated at 600 °C in air for 6, 12, 18, and 24 h after a 20-min MAO process on hot-dip aluminized titanium.  $\text{Al}_3\text{Ti}$  peaks appeared after over 12 h of annealing, whereas the alumina phase peaks remained unchanged throughout. The aluminum coating presented in Fig. 11 partially (not completely) transformed into an intermetallic compound layer, which EDS confirmed to be  $\text{Al}_3\text{Ti}$ . In solid diffusion reactions,  $\text{Al}_3\text{Ti}$  is usually the only observed phase at the Ti/Al interface; the much faster diffusivity of the  $\text{Al}_3\text{Ti}$

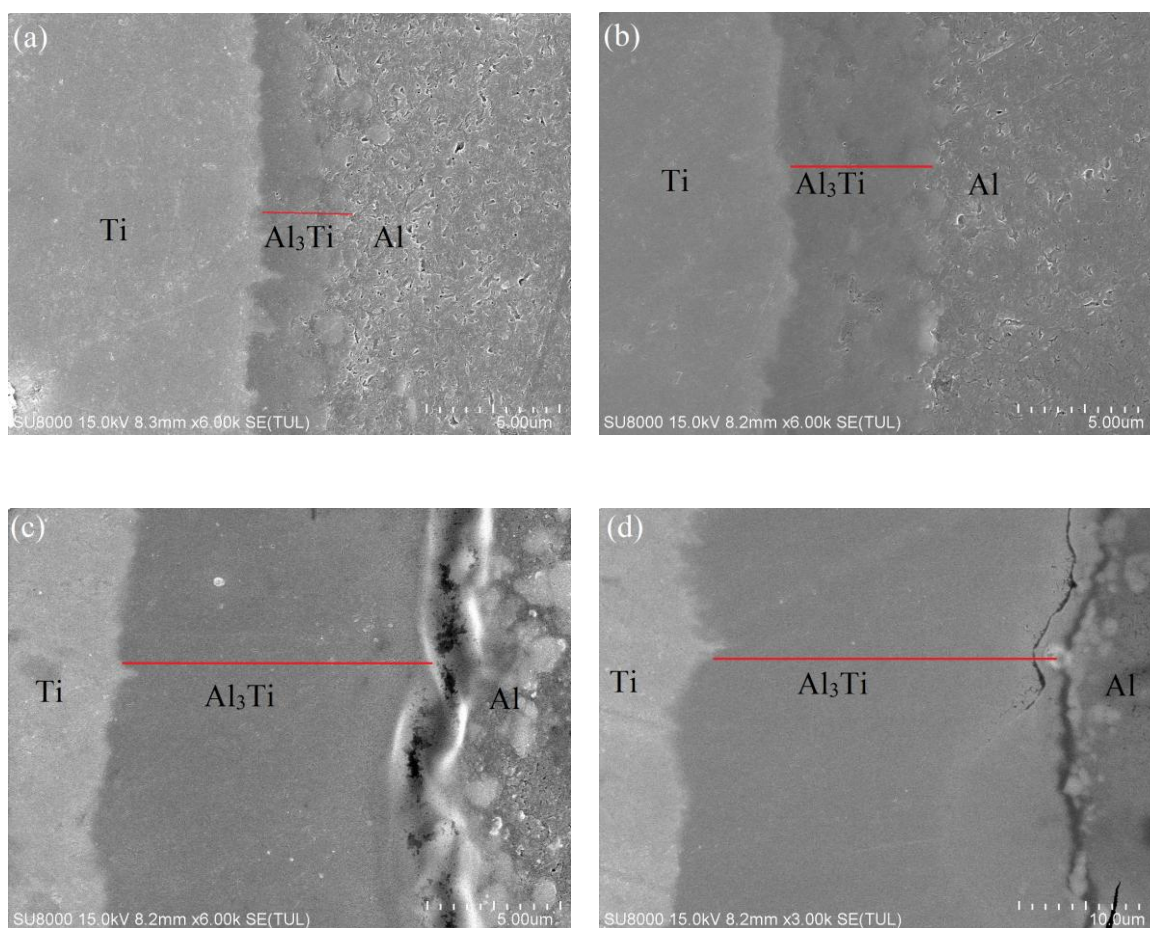
compound accounts for the absence of all other phases [22]. In the cross-sectional SEM image of the coating,  $\text{Al}_3\text{Ti}$  is approximately 3  $\mu\text{m}$  thick for 6 h, 5.6  $\mu\text{m}$  for 12 h, 11  $\mu\text{m}$  for 18 h, and 27  $\mu\text{m}$  for 24 h of annealing, respectively, indicating that the growth of the  $\text{Al}_3\text{Ti}$  layer increases geometrically with annealing duration. However, after 18 h of annealing, cracks appeared at the interface of the  $\text{Al}_3\text{Ti}$  layer and the Al coating because the  $\text{Al}_3\text{Ti}$  compound is brittle [23]; volume shrinkage of nearly 6% was caused by the growth of the  $\text{Al}_3\text{Ti}$  layer transformed by the Al coating and the pure titanium substrate. The corrosion properties of the annealed 20-min MAO coatings are shown in Table 3. The corrosion current density increased with the annealing duration. The  $\text{Al}_3\text{Ti}$  layer is conspicuously harmful to the corrosion resistance of the sample. The highest corrosion current density was observed after 18 h of annealing, because 18-h samples had the largest cracks. This poorer corrosion resistance may be attributable to the pores, or cracks induced by the collection of pores, at the interface of the  $\text{Al}_3\text{Ti}$  layer and Al coating in the annealed sample. In other words, cracks in the  $\text{Al}_3\text{Ti}$  layer, arising from the volume shrinkage caused by  $\text{Al}_3\text{Ti}$  formation, caused the poor corrosion resistance. Therefore, minimizing the thickness of the intermediate compound layer is essential for improving corrosion resistance.



**Figure 10.** XRD patterns for hot-dip aluminized titanium formed through MAO for 20 min, followed by annealing at 600 °C for (a) 0 h, (b) 6 h, (c) 12 h, (d) 18 h, and (e) 24 h.

**Table 3.** Corrosion properties of the annealed MAO coatings formed for 20 min.

Diffusion time (h)	Corrosion potential (V)	Corrosion current density ( $A/cm^2$ )
0	-0.468	$2.39 \times 10^{-9}$
6	-0.805	$3.26 \times 10^{-8}$
12	-0.804	$4.13 \times 10^{-7}$
18	-0.659	$7.82 \times 10^{-7}$
24	-0.756	$3.37 \times 10^{-7}$

**Figure 11.** SEM micrographs of coating cross sections of hot-dip aluminized titanium formed through MAO for 20 min, followed by annealing at 600 °C for (a) 6 h, (b) 12 h, (c) 18 h, and (d) 24 h.

#### 4. CONCLUSIONS

1. A multilayer structure comprising ceramic, aluminum, and intermetallic compound layers and a titanium substrate was synthesized using MAO on aluminized titanium. This multilayer coating exhibits high hardness, acceptable corrosion resistance, and extraordinary wear resistance.

2. The thickness of the Al<sub>2</sub>O<sub>3</sub> layer initially steadily increased with the MAO duration. However, the thickness of the MAO coatings leveled off slowly at prolonged MAO durations.

3. The MAO coatings were dense and uniform and were mainly composed of  $\alpha$ -Al<sub>2</sub>O<sub>3</sub> and  $\gamma$ -Al<sub>2</sub>O<sub>3</sub>. Their surface hardness increased with the MAO duration. The soft titanium substrate contributes to the low hardness in samples with thin MAO coatings, such as those formed for 10 min. The hardness of the Al<sub>2</sub>O<sub>3</sub> layer increased with the MAO duration because the  $\alpha$ -Al<sub>2</sub>O<sub>3</sub> phase increased in the layer with the MAO duration.

4. The wear resistance of the MAO coatings can be considerably improved by increasing the MAO duration, which results in thicker coatings. The MAO sample formed through 40 min of MAO offered the highest wear resistance. However, the sample formed for 20 min exhibited the highest corrosion resistance in a 3.5 wt.% NaCl solution.

5. After diffusion annealing, cracks in the Al<sub>3</sub>Ti layer, arising from the volume shrinkage caused by Al<sub>3</sub>Ti formation, caused the corrosion resistance to be poor.

#### ACKNOWLEDGEMENTS

The authors are sincerely grateful for the financial support from Tatung University under Grant No. B101-T10-069.

#### References

1. C. Martinia, L. Ceschini, F. Tarterini, J.M. Paillard and J.A. Curran, *Wear*, 269 (2010) 747
2. M. Khorasani, A. Dehghan, M.H. Shariat, M.E. Bahrololoom and S. Java, *Surf. Coat. Tech.*, 206 (2011) 1495
3. A. Banerji, S. Bhowmick and A.T. Alpas, *Surf. Coat. Tech.*, 241 (2014) 93
4. J.C. Avelar-Batista, E. Spain, G.G. Fuentes, A. Sola, R. Rodriguez and J. Housden, *Surf. Coat. Tech.*, 201 (2006) 4335
5. Y.X. Leng, J.Y. Chen, P. Yang, H. Sun and N. Huang, *Surf. Coat. Tech.*, 166 (2003) 176
6. J.M. Wheeler, C.A. Collier, J.M. Paillard and J.A. Curran, *Surf. Coat. Tech.*, 204 (2010) 3399
7. V.S. Rudnev, *Surf. Coat. Tech.*, 235 (2013) 134
8. C.-J. Hu, J.-L. Lee, C.-Y. Lu, Y.-C. Lin and M.-R. Yang, *ECS Trans.*, 33(30) (2011) 39
9. C.-C. Tseng, J.-L. Lee, T.-H. Kuo, S.-N. Kuo and K.-H. Tseng, *Surf. Coat. Tech.*, 206 (2012) 3437
10. Y. Gao, X. Xu, Z. Yan and G. Xin, *Surf. Coat. Tech.*, 154 (2002) 189
11. M. Zandrahimi, J. Vatandoost and H. Ebrahimifar, *Oxid. Met.*, 76 (2011) 347
12. G. H. Awan and F. U. Hasan, *Materials Science and Engineering A*, 472 (2008) 157
13. J.-H. Kim, J.-P. Wang and C.-Y. Kang, *Met. Mater. Int.*, 17(6) (2011) 931
14. J. Mackowiak and L. L. Shreir, *J. Less-Common Met.*, 1 (1959) 456
15. Y.S. Wang, J. Xiong, J. Yan, H.Y. Fan and J. Wang, *Surf. Coat. Tech.*, 206 (2011) 1277
16. D. Wang, Z. Shi and Y.L. Teng, *Appl. Surf. Sci.*, 250 (2005) 238
17. S. Xin, L. Song, R. Zhao and X. Hu, *Thin Solid Films*, 515 (2006) 326
18. C.-J. Hu and M.-H. Hsieh, *Surf. Coat. Tech.*, 258 (2014) 275
19. Y.-L. Chenga, Z.-G. Xue, Q. Wang, X.-Q. Wu, E. Matykina, P. Skeldon and G.E. Thompson, *Electrochim. Acta*, 107 (2013) 358
20. W. Xue, C. Wang, R. Chen and Z. Deng, *Mater. Lett.*, 52 (2002) 435

21. A. Bai, P.-Y. Chuang and C.-C. Hu, *Mater. Chem. Phys.*, 82 (2003) 93
22. F. J. J. van Loo and G. D. Ricek, *Acta Metallurgica*, 21(1973) 61
23. H. P. Xiong, Q. Shen, J. G. Li, L. M. Zhang and R. Z. Yuan, *J. Mater. Sci. Lett.*, 19 (2000) 989

© 2015 The Authors. Published by ESG ([www.electrochemsci.org](http://www.electrochemsci.org)). This article is an open access article distributed under the terms and conditions of the Creative Commons Attribution license (<http://creativecommons.org/licenses/by/4.0/>).